

We are IntechOpen, the world's leading publisher of Open Access books Built by scientists, for scientists

6,900

Open access books available

186,000

International authors and editors

200M

Downloads

Our authors are among the

154

Countries delivered to

TOP 1%

most cited scientists

12.2%

Contributors from top 500 universities



WEB OF SCIENCE™

Selection of our books indexed in the Book Citation Index
in Web of Science™ Core Collection (BKCI)

Interested in publishing with us?
Contact book.department@intechopen.com

Numbers displayed above are based on latest data collected.
For more information visit www.intechopen.com



Electrodeposition Approaches to Deposit the Single-Phase Solid Solution of Ag-Ni Alloy

*Brij Mohan Mundotiya, Wahdat Ullah
and Krishna Kumar*

Abstract

The Ag-Ni films have attracted the attention of material scientists and researchers due to its applications as magnetic materials, catalyst, optical materials, etc. In the bulk, the formation of a single-phase solid solution of the Ag-Ni alloy film is difficult due to the large differences in the atomic size and the positive enthalpy of mixing. However, the immiscibility in the Ag and Ni constituents is diminished in the nano-sized level. The electrodeposition method has established itself as a most suitable method for synthesis of single-phase Ag-Ni alloy films due to its time efficiency, cost-effectiveness, and ability to mass production of single-phase solid solutions. In this method, the miscibility of alloying elements (i.e., Ag and Ni) and the quality of the Ag-Ni film can also be easily controlled by tuning the electrodeposition process parameters such as the magnitude of the applied current density, temperature of the electrolyte, additives in electrolytes, etc. This chapter presents a detailed overview of the process parameters affecting the miscibility, morphology, and the quality of the single solid solution of Ag-Ni film. Furthermore, the nucleation and growth mechanism of Ag-Ni film and the effect of the curvature of the deposited film's particles in the miscibility of the Ag and Ni elements have also been discussed in detailed.

Keywords: deposition parameters, electrodeposition, immiscibility, morphology, single-phase Ag-Ni alloy

1. Introduction

In recent years, the researchers are looking with the hope that the metastable (non-equilibrium) alloys might be materials with potentially unique and exploitable functional properties. The alloys in the non-equilibrium state are generally made from the immiscible element system such as Co-Ag, Ag-Ni, Au-Co, Ag-Pt, Fe-Cu, Co-Cu, and Ag-Fe alloy systems. In bulk state, constituent elements of these systems exhibit strong immiscibility behavior even up to very high temperatures. However, miscibility of their constituent elements can be enhanced by mixing them in nanoscale level to form a nano-size system. The enhanced miscibility of constituent elements in the nano-size system also induces its exploitable functional properties due to the evolution of the unique type of microstructure [1]. In recent years, numerous amorphous and nanocrystalline single solid solution alloy systems of immiscible elements Ni-Co [2], Ni-W [3], Ni-Si [4], and Ni-Fe [5, 6] have all been explored and

reported in scientific literatures. Among the metastable alloys systems, Ag-Ni alloy system is one of the very interesting system due to the presence of one magnetic (Ag) and one nonmagnetic (Ni) alloying elements and their possible applications in the field of catalysts [7], magnetic materials [8, 9], electrical materials [10], and optical materials [11]. But due to the alloying characteristics of the constituent elements of the Ag-Ni system, these systems have been explored very little.

The alloying elements of Ag-Ni system (i.e., Ag and Ni elements) have the same lattice structure (FCC), and the difference between their atomic sizes is very large (~14%). They are immiscible in both the solid and liquid states or even up to very high temperatures. The phase diagram of the Ag-Ni system is very simple (see **Figure 1**). As it is obvious from the phase diagram that Ag and Ni are mutually insoluble, even at 400°C, the solubility of Ni in Ag is only ~0.0219 at% [12]. The reasons of the high immiscibility of Ag and Ni alloying elements are (a) the large difference in their atomic sizes (~14%) and (b) a positive enthalpy of mixing (ΔH^{mix} for solid solution equiatomic Ag-Ni alloy is 23 kJ/mol) [13, 14]. However, an enhancement of miscibility between Ag and Ni atoms in nano-size level to form a nano-size system has been achieved by researchers [8–11]. Enhancement of miscibility of atoms of nanoparticles of Ag and Ni can be attributed to (a) the effect of increase of particles curvatures with the reduction of their sizes that facilitate miscibility in accordance with the Gibbs-Thomson effect and (b) the decrease of the driving force for the nucleation and growth of the second phase within a nano-sized particle [13].

In recent years, the single-phase Ag-Ni alloys have successfully synthesized by various techniques such as ion beam mixing [16], laser ablation [10], gamma-ray irradiation [17], etc. Zhang et al. [17] synthesized the single solid solution phase of Ag-Ni alloy by simultaneous reduction of Ag and Ni ions by gamma-ray irradiation. The authors obtained a single solid solution phase of the Ag-Ni system with the homogeneous distribution of compositions of Ag and Ni atoms inside the particles. The average size of the particle of a single solid solution of Ag-Ni system

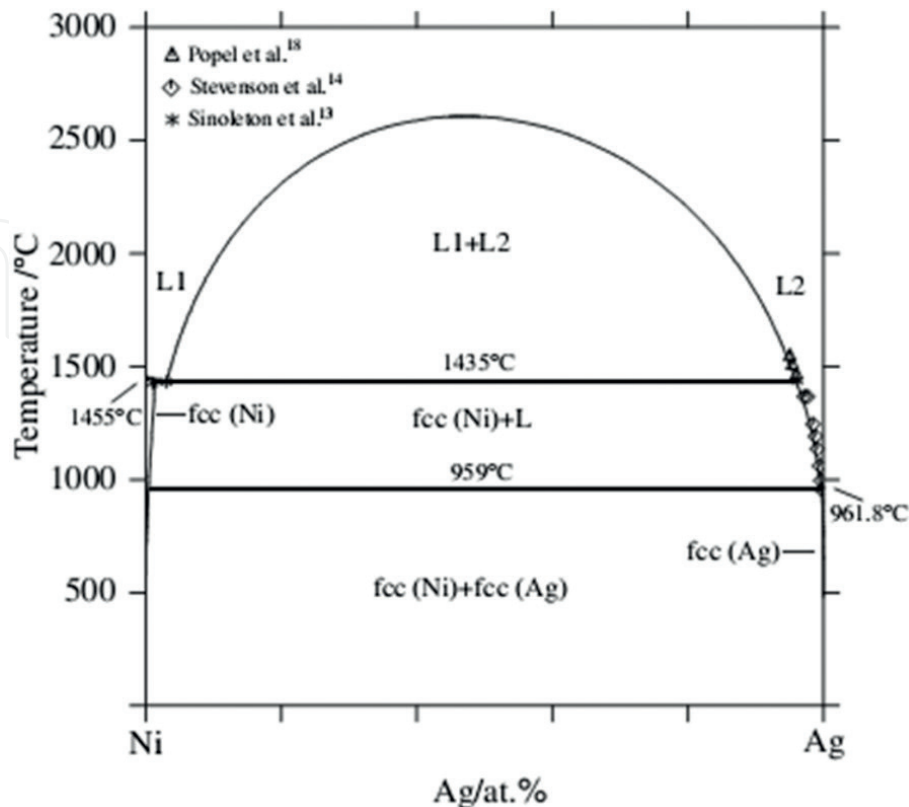


Figure 1.
Phase diagram of Ag-Ni system [15].

was 6 nm. In another study reported by Kumar et al. [18], an average particle size of 30 nm of a single solid solution of Ag-Ni system was synthesized by immersion of a film of thermally evaporated fatty acids sequentially in solutions containing Ag^+ ions and Ni^+ ions. Srivastava et al. [19] studied the size-dependent microstructural evolution for Ag-Ni alloy nanoparticles. The authors synthesized Ag-Ni nanoparticles by the co-reduction of Ag and Ni metal precursors. It was found that the Ag and Ni atoms were completely mixed in Ag-Ni alloy nanoparticles when the particle size was less than 7 nm. As the size of the particles was increased, the nanoparticles showed two separate regions: (a) a pure Ag region and (b) a solid solution of Ag-Ni alloy.

The electrodeposition method has established itself as a most suitable method for synthesis of single-phase Ag-Ni alloy films due to its time efficiency, cost-effectiveness, and ability to mass production of single-phase solid solutions [13, 20–26]. In the electrodeposition process, the apparatus used for the deposition of the film is less complicated than the vacuum-based methods such as molecular beam epitaxy or sputtering. In this method, miscibility of the alloying elements (Ag and Ni) to form a single-phase solution of Ag-Ni films and their quality can also be easily controlled by tuning the electrodeposition process parameters such as current density, electrolytes, electrolyte temperatures, additives in electrolytes, etc. In the following sections of this chapter, the overview of information related to the effects of these parameters on the miscibility of the alloying elements (Ag and Ni) and the quality of the deposited film are discussed.

2. Nucleation and growth mechanism of film

The deposition of the alloy films on the conductive substrate involves the nucleation and growth process. The nucleation process is very important because it decides the nature of the evolution of microstructure and crystallinity in the deposited alloy film. The alloy film deposition on the conductive substrate by electrodeposition method involves a heterogeneous process. The interface between the electrolyte solution and the substrate surface provides preferential sites for nucleation. As an example, consider the nucleation of a nucleus on the substrate surface (see **Figure 2**). On the substrate surface, nucleus forms in the shape of a half convex lens (spherical cap). The surface tension force acting on the surface-nucleus-electrolyte interfaces is determined by the formula given in Eq. (1). This equation is known as Young's equation [27]:

$$\gamma_{sl} = \gamma_{fs} + \gamma_{lf} \cos\theta \quad (1)$$

where γ_{lf} , γ_{fs} , and γ_{sl} are the surface or interface energy of electrolyte-nucleus, nucleus-substrate, and substrate-electrolyte interfaces, respectively, and θ is the contact angle that depends on nature of the surfaces involved to form interfaces.

In the heterogeneous nucleation process, the probability of the nucleation is determined by the critical nucleus radius r^* and the activation energy barrier ΔG^* that a nucleation process must be overcome to form a nucleus. The formulae for the r^* and ΔG^* are given by Eqs. (2) and (3), respectively [28]:

$$r^* = \left(\frac{2\pi\gamma_{lf}}{\Delta G_l} \right) \left(\frac{\sin^2\theta \cdot \cos\theta + 2\cos\theta - 2}{2 - 3\cos\theta + \cos^3\theta} \right) \quad (2)$$

$$\Delta G^* = \frac{16\pi\gamma_{lf}}{3(\Delta G_l)^2} \left(\frac{2 - 3\cos\theta + \cos^3\theta}{4} \right) \quad (3)$$

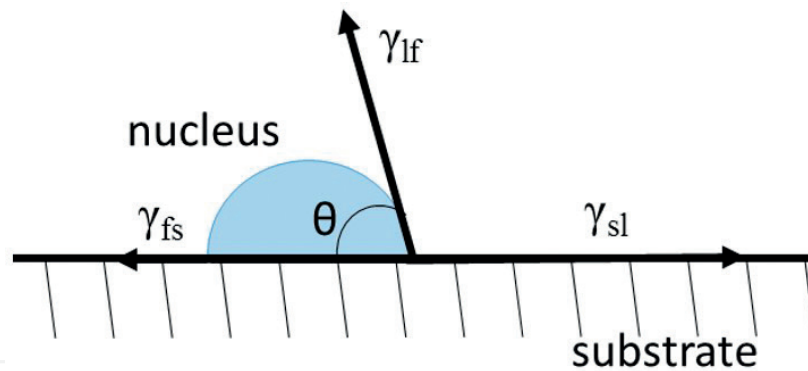


Figure 2. Schematic diagram of a nucleus on a solid surface (substrate) with energy vectors and contact angle.

where ΔG_v is the Gibbs free change per unit volume. If the radius (r) of the nucleus is smaller than the critical nucleus radius (r^*), the nucleus is not survived for further growth and redissolved.

From the atomic point of view, the electrodeposition of film occurs in two different stages. In the first stage, few metal atoms from the electrolyte solution adhere to the substrate. Normally, it is considered that the first stage may process via either of the two mechanisms: (a) step-edge site ion transfer or (b) terrace site ion transfer [29]. In the step-edge site ion-transfer mechanism, the metal adions transfer from the electrolyte solution to a kink site of a step edge of the substrate surface via two paths. In the first path, the metal adions directly transfer from the electrolyte solution to the kink site of a step edge of the substrate. While in the second path, the metal adions diffuse from the electrolyte solution to the step edge first and then finally transfer to the kink site. On the other hand, in the terrace ion-transfer mechanism, the metal adions transfer from the electrolyte solution to the flat surface of the terrace region. The bonds between the metal adions are stronger to each other than to the surface of terrace regions. Therefore, metal adions easily diffuse from the terrace and transfer to the step-edge site and then finally to a kink site. These clusters of metal adions on the different sites of the substrate form nuclei of ordered structure.

Following the first stage, the second stage of growth of the nucleus occurs. The experimental observations revealed that there are three basic kinds of growth modes of alloy film [30]: (a) island growth, (b) layer growth, and (c) island-layer growth. When the bond between the depositing species (i.e., metal adions) is stronger than to the substrate, the island growth occurs. As the deposition proceeds, the islands of deposit subsequently grow and merge to form a continuous film on the substrate. The layer growth of film occurs, when the depositing species (i.e., metal adions) are bound strongly to the substrate than to each other. In the layer growth mode, first of all, a complete monolayer of depositing species is formed on the substrate, then a second layer starts to deposit on the monolayer. The island-layer growth mode of alloy film is a combination of both island and layer growth modes. In the island-layer growth mode, first of all, a layer of deposit is grown on the substrate by the layer growth mechanism; this layer has some degree of residual stresses when the critical thickness of the layer is reached then due to an increase of the stresses on it, the island growth mechanism is activated.

3. Electrodeposition solution for Ag-Ni films

Metastable Ag-Ni alloy films are deposited by electrodeposition method by using their respective salts and some additives (such as thiourea, saccharin, trisodium

Coating/ nano- particles	Electrolyte bath	pH	Temperature (°C)	Current density (mA/ cm ²)	Substrate	Reference
Ag-Ni film	C ₆ H ₅ Na ₃ O ₇ : 0.3 M NiSO ₄ : 0.7 M AgNO ₃ : 2–5 mM	4.5– 7.5	Room temperature	0.5–50	Brass plate	Eom et al. [20]
Ni-Ag coating	NiSO ₄ ·6H ₂ O: 49.93 g/L AgNO ₃ : 0–0.339 g/L C ₆ H ₅ Na ₃ O ₇ ·2H ₂ O: 0–41.160 g/L H ₃ BO ₃ : 12 g/L	5.6	30	5	Cu plate	Raghupathy et al. [21]
Ni-Ag layer	C ₆ H ₅ Na ₃ O ₇ : 0.26 mol/L NiSO ₄ : 0.7 mol/L AgNO ₃ : 0.002 mol/L	5.5	Room temperature	—	Cu plate	Schneider et al. [22]
Ag-Ni film	AgClO ₄ : 0.01 M Ni(ClO ₄) ₂ : 0.15 M NaClO ₄ : 0.1 M H ₃ BO ₃ : 0.15 M Thiourea: 0.2 M	3	—	—	Cu sheet	Liang et al. [23]
Ag-Ni film	AgNO ₃ : 0.01 M Ni(NO ₃) ₂ ·6H ₂ O: 0.08 M H ₃ BO ₃ : 0.003 M Thiourea: 0.045 M	3.2	Room temperature	25	Cu plate	Srivastava et al. [24]
Ag-Ni solid film	AgNO ₃ : 1.69 g Ni(NO ₃) ₂ ·6H ₂ O: 0.25 g H ₃ BO ₃ : 0.02 g in 100 mL distilled water	12	Room temperature	100	Cu plate	Srivastava et al. [25]
Ag-Ni nano particles	AgNO ₃ : 1.69 g Ni(NO ₃) ₂ ·6H ₂ O: 0.25 g H ₃ BO ₃ : 0.03 g Thiourea: 0.35 g in 100 mL distilled water	3.6	80	20, 70, and 100	Cu plate	Srivastava et al. [26]

Table 1.
 Electrodeposition parameters used for the deposition of Ag-Ni alloy films/nanoparticles.

citrate, citric acid, sodium perchlorate, etc.). The electrolyte is the electrochemical solution of metal or alloy salts that is required to deposit at cathode (conductive substrate) surface during electrolysis. The deionized and distilled waters are used as a solvent for most of the electrolytes; therefore, these electrolytes are called aqueous electrolytes. The costs of the aqueous electrolytes are lesser than the nonaqueous electrolytes due to the easy availability of the water solvent. Deionized water is water that has been treated to remove all the dissolved mineral salts. While, the distilled water is prepared by boiling the normal water so that it evaporates and then recondensed, leaving most impurities behind [31].

Mostly sulfate and nitrate salts with some suitable additives (such as thiourea, saccharin, trisodium citrate, citric acid, sodium perchlorate, etc.) are used for the preparation of the electrolytes for deposition of the Ag-Ni systems. The sulfate and nitrate salts have high solubility in the water. The additives in the electrolyte act as grain refiners, complexing agents, brighteners, etc. The additive of sodium perchlorate is commonly used for reducing the resistance (i.e., viscosity) and increasing the ionic conductivity of the electrolytes [32]. And for improving quality of Ag in the deposited film, additives of boric acid and sodium gluconate are generally added in the electrolyte [33, 34].

List of some typical salts of metal ions with and without additives which are often used for deposition of Ag-Ni films/nanoparticles and the involved deposition process parameters are shown in **Table 1**.

4. Electrodeposition parameters for the Ag-Ni alloy films

The solid solubility, structure, and morphology of the deposited Ag-Ni alloy films depend on the several electrodeposition process parameters. Some of the crucial process parameters influencing the miscibility, morphology, and structure of the Ag-Ni alloy films are discussed in given below subsections.

4.1 Deposition current density

According to the electro-crystallization theory, whenever a high current density is applied, a high overpotential is generated at the cathode, as a consequence of this, the nucleation rate increases. The faster nucleation rate reduces the particle sizes of the deposited film [35–39], because the fine particle sizes increase the specific area or curvature that promotes the miscibility of the constituent elements [40, 41]. This phenomenon is known as the Gibbs-Thomson effect.

The composition of the Ag-Ni alloy film could be altered by changing the current density. Santhi et al. [32] have deposited metastable Ag-Ni film with the granular kind of morphology. The average particle size was ~50 nm. They observed that the Ni content in the deposited Ag-Ni film increases with increasing current densities. Bdikin et al. [42] reported that the particle size of the deposited Ag-Ni film decreases with increasing Ni contents in the film. For 70 wt% of Ni content, the Ag-Ni film particle size goes down to very small (~3.3 nm). Eom et al. [20] investigated the effect of the current density on the chemical composition and crystallography of the deposited Ag-Ni film. They deposited Ag-Ni films on a brass substrate using NiSO_4 , AgNO_3 , and $\text{C}_6\text{H}_5\text{Na}_3\text{O}_7$ electrolyte. The Ag content in the deposited Ag-Ni film was found to be higher at lower current density. The high content of Ag in the deposited film was due to its lower reduction potential. However, the content

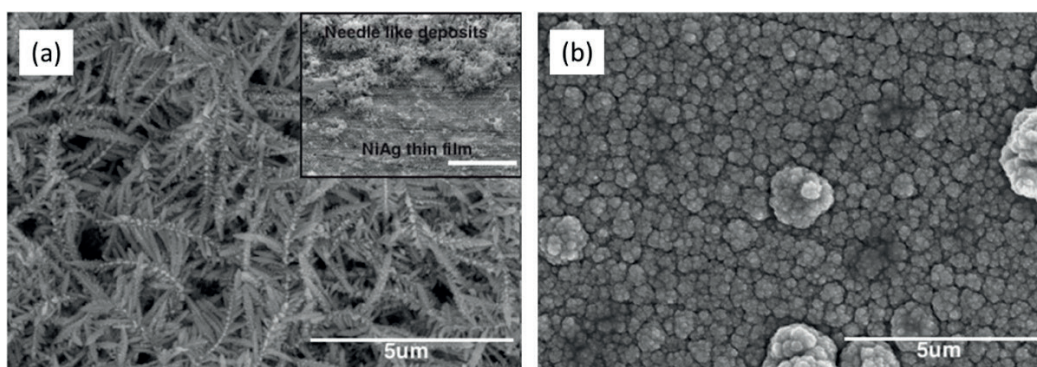


Figure 3. SEM micrographs of Ag-Ni films deposited at current densities of (a) 0.5 mA/cm^2 and (b) 10 mA/cm^2 [20].

of Ni in the deposited films was found to be increased with increasing current density. At higher current density, Ni becomes the dominant component because of the more transfer limitation of Ag ions. Apart from the change in composition, the change in morphology as well as the grain size of the films with changing current densities was also reported by the authors. At a current density of 0.5 mA/cm², films had dendritic kind of morphology. But when the current densities were increased from 0.5 to 50 mA/cm², the morphologies were changed from dendritic to particle type (see **Figure 3**), and a significant reduction in grain sizes had also occurred.

The enhancement of miscibility of Ag and Ni elements to form a single-phase solid solutions of Ag-Ni alloy systems can be explained by Tafel equation (Eq. (4)) [43] and Eq. (5) [20] given below:

$$\eta = a + b \log i \quad (4)$$

$$J = K_1 \exp\left(\frac{-gs\varepsilon^2}{zekT\eta}\right) \quad (5)$$

where η is the overpotential at cathode, a and b are the constants, i is the current density, J is the nucleation rate, K_1 is the rate constant, g is the factor relating the surface area S of the nucleus to the perimeter P ($g = P^2/4S$), s is the area occupied by one atom on the surface of the nucleus, T is the electrolytic temperature, k is the Boltzmann constant, and z , e , and ε are the number of electrons involved in the reaction, electron charge, and edge energy, respectively. According to Tafel equation (Eq. (4)), the reduction in the grain size is primarily due to the increase in the overpotential by increasing the current density. The relations between the nucleation rate, overpotential, and current density are given by Eqs. (4) and (5). From Eq. (5), it is clear that the nucleation rate has an exponential relationship with the overpotential. As the overpotential at the cathode increases, the nucleation rate also increases exponentially. In Eqs. (4) and (5), it can also be seen that the nucleation rate and current density are related to each other. Therefore, when current density increases, the overpotential at the cathode increases, as a result of this, the nucleation rate also increases. The increase in the nucleation rate produces finer grains in the deposited film. The finer grains increase the specific area or curvature which promotes an increase in the extent of miscibility of Ag and Ni atoms to form a single solid solution of Ag-Ni system.

Srivastava and Mundotiya [26] investigated the influence of the current density on the particles size of the deposited Ag-Ni alloy films. The Ag-Ni films were deposited on the Cu-substrate (30 mm X 10 mm X 0.3 mm) by using the electrolyte (0.17 g of AgNO₃, 0.25 g of Ni(NO₃)₂•6H₂O, 0.03 g of H₃BO₃, and 0.35 g of thiourea in 100 ml of distilled water (pH ~ 3.6). During the electrodeposition, the temperature of the electrolyte was maintained at 80°C. The addition of an additive (complexing agent) of thiourea was chosen to deposit a granular kind of morphology in Ag-Ni film. They observed no significant change in morphologies of the deposited Ag-Ni films at current 20, 70, and 100 mA. At these current densities, the morphologies of the deposited films were similar granular morphology. However, the content of Ni in the Ag-Ni films increases, while the sizes of grains decrease with increasing current densities. These trends were in agreement with those reported in the scientific literature [20, 32, 42]. Thus, as a general statement, it can be concluded that the decrease in the grain size of the Ag-Ni film increases the miscibility of the constituent elements.

The miscibility behavior of the Ag-Ni system with different contents of Ni in Ag-Ni films can be explained by the X-ray diffraction (XRD) patterns shown

in **Figure 4**. It can be seen in the patterns that the peaks of the Ag-Ni films shift to higher angles with increasing Ni content. The shifting of the peaks indicates substitution of the more Ag atoms by the relatively smaller Ni atoms with increasing content of Ni. That means the lattice constant of the Ag-Ni films decreases with increasing content of Ni. As the lattice constant decreases, the interplanar spacing of the Ag-Ni alloy films also decreases because the lattice constant is directly proportional to the interplane spacing. And the interplanar spacing is inversely proportional to the angle. Another important characteristic showed by the XRD profile is the broadening of the Ag-Ni films peaks with increasing Ni content. The broadening could be the result of decreasing grain size of the Ag-Ni films with increasing Ni content.

Therefore, the current density is the important parameter to control the miscibility of the Ag-Ni alloy system by controlling the size and composition.

4.2 Electrolyte temperature

The temperature of the electrolyte also influences the morphologies, the particles sizes, and the quality of the deposited single solid solution of the Ag-Ni films. This is due to the fact that the solubility of the metal salts in the electrolyte can be sufficiently increased by increasing the temperature of the electrolyte. As the temperature increases, the viscosity of the electrolyte decreases, and as a result of this, the mobility (diffusion and migration) of the metal ions toward the cathode increases [36]. Due to an increase in solubility and mobility of the metal ions in the electrolyte at a higher temperature, the conductivity of the electrolytes also improves, because the conductivity of the electrolyte depends on the degree of dissociation of dissolved metal ions in the electrolyte and the mobility of dissolved metal ions. The improvement in the conductivity of electrolyte at higher temperature decreases the overpotential at the cathode [44, 45]. A decrease in the cathodic overpotential with an increase in the electrolyte temperature above 55°C is reported by Rashidi and Amadeh [46]. The decrease in the cathodic overpotential slows down the nucleation rate; at low nucleation rate, the existing nuclei grow faster.

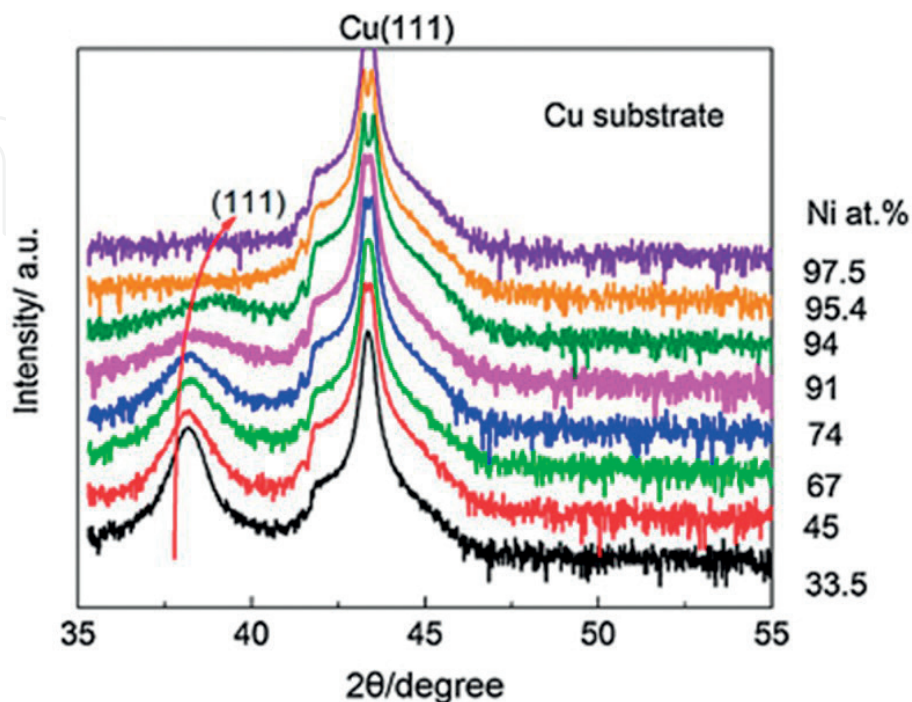


Figure 4. XRD pattern of Ag-Ni alloy films with different Ni-content [23].

Thus it can be concluded that an increase in the temperature of the electrolyte may lead to increased particle/grain growth in the deposited Ag-Ni film [26, 46, 47].

The temperature of the electrolyte also influences the composition of the deposited film. The concentration of Ag in the deposited film increases with increasing electrolyte temperature [48]. To deposit the films of the same compositions at different electrolyte temperatures, very high overpotential at the cathode is required. But high overpotential at the cathode favors hydrogen evolution which is undesirable for deposition of high-quality alloy film because it creates pores and/or hydrogen embrittlement in the deposit films [48].

4.3 Additives

The addition of the suitable additives in the electrolyte affects the morphology and the quality of the deposited film. The additives in the electrolyte produce an additional overpotential at the cathode [36] which helps in the creation of a homogeneous film with a low level of roughness [49]. For improving the quality of the deposited film, many suggestions have been given by the researchers. Among those suggestions, the most common suggestion is related to the blocking of lattice sites by adsorption of additives on the surface of the substrate. This helps to prevent the growth of grains in the deposited film by inhibiting short-range surface diffusion [50].

The reduction of Ag and Ni takes place at a potential of +0.2 and -0.26 V, respectively. The difference between the reduction potentials of Ag and Ni is too large. Due to the existence of this large difference in the reduction potentials of Ag and Ni during electrodeposition of Ag-Ni film, morphological instabilities between Ag and Ni phases occur during the growth process of the Ag-Ni film. Therefore, synthesizing a perfect Ag-Ni film by co-deposition of Ag and Ni is difficult in this condition. The deposited Ag-Ni film generally has a porous and dendritic morphology. For minimizing the difference of the reduction potentials of Ag and Ni, some suitable additives such as sodium citrate ($C_6H_5Na_3O_7$), thiourea, etc. are commonly added with electrolyte [20, 34]. The morphology of the electrodeposited Ag-Ni film can be tuned by the addition of suitable additives and/or complexing agents in the electrolyte. These additives shift the reduction potentials of Ag and Ni more closely. The thiourea is one of the additives which has a strong complexing capacity with Ag [41] but no or weak complex with Ni. Due to its strong complexing capacity with Ag, it decreases the reduction potential of Ag into more negative potential without altering the reduction potential of Ni. The minimization of the difference of the reduction potentials of Ag and Ni by addition of additive in electrolyte also helps in suppressing the evolution of the hydrogen at the cathode. After the addition of the additive of thiourea in the electrolyte solution, a change of morphology of the feature of the deposited Ag-Ni films is observed [51]. The dendritic morphology changes to nanoparticles by adding additives in the electrolyte solution as shown in SEM micrographs in **Figure 5**. This transformation of dendritic morphology into nanoparticles after addition of thiourea additive in the electrolyte solution can be attributed to the minimization of the difference of the reduction potentials of the Ag and Ni elements.

The decrease of the reduction potential of Ag by adding additive of thiourea in the electrolytic solution is also reported by Liang et al. [23]. They deposited Ag-Ni films on the Cu substrate by using thiourea-based acidic solutions as an electrolyte. It was observed that the presence of thiourea in the electrolyte decreases the reduction potential of Ag via formation of the metal-organic complex. The average grain size in the deposited film was found to be lesser than 200 nm. It was also detected that the deposited films consist of a mixture of various phases such as a supersaturated solid solution of Ag-rich phase, pure Ni phase, and an amorphous phase at the boundaries. These phases were metastable. However, when the Ag-Ni

alloy films were annealed at 600°C, these metastable phases were separated into Ag phase and Ni phase. Bdikin et al. [42] have also confirmed the separation of supersaturated solid solution (metastable phase) of Ag-Ni film into a single elemental phase after annealing the film at 600°C. They deposited the Ag-Ni films of different compositions on the copper substrates by using a single electrolyte containing Ag and Ni ions at room temperature and the current density 2–5.4 mA/cm². The authors detected that the deposited nanocrystalline Ag-Ni films were metastable. These deposited Ag-Ni films become unstable with increasing annealing temperatures and decompose into a single elemental phase when annealed at 600°C.

4.4 Curvature of the deposited film's particles

The curvature provided by the particles of the deposited films is also playing a very crucial role in increasing the miscibility of the constituent elements. Srivastava and Mundotiya [25] explored the possibility of changes in the extent of miscibility of Ag and Ni elements with changes in the system's morphology and tried to establish a correlation between size, morphology, and extent of miscibility in the Ag-Ni system. They deposited the Ag-Ni alloy films on the Cu substrate (30 mm × 10 mm × 0.3 mm) by using the electrolyte solution (1.69 g of AgNO₃, 0.25 g of Ni(NO₃)₆H₂O, and 0.02 g of H₃BO₃ in 100 mL of distilled water) at the current input of 100 mA and deposition time of 10 minutes. It was observed that the Ag-Ni films contain features of two distinct morphologies: (a) dendritic morphology (designated by type A feature) and (b) branched wire type morphology (designated by type B feature), as can be seen in **Figure 6(a)** and **(b)**, respectively. The dendritic morphology (i.e., type A feature) had high Ag content in single-phase Ag-Ni when compared to the branched wire type morphology (i.e., type B of the feature). The SAED pattern from the type A feature shows a regular array of diffraction spots, which indicates that the dendritic morphology is a single crystal with size in micrometer range (**Figure 6(c)**), while the SAED pattern from the region of the type B feature consists of series of concentric rings, which indicates that the wire type morphology is polycrystalline in nature, and contains a large number of nanoparticles, and the rings in SAED pattern result in falling of the sum of individual patterns of these particles on the concentric rings (**Figure 6(d)**). The SAED patterns (both from the regions of the type A and type B features) did not show any diffraction for Ag, Ni, or even their oxides. The measured d-spacing

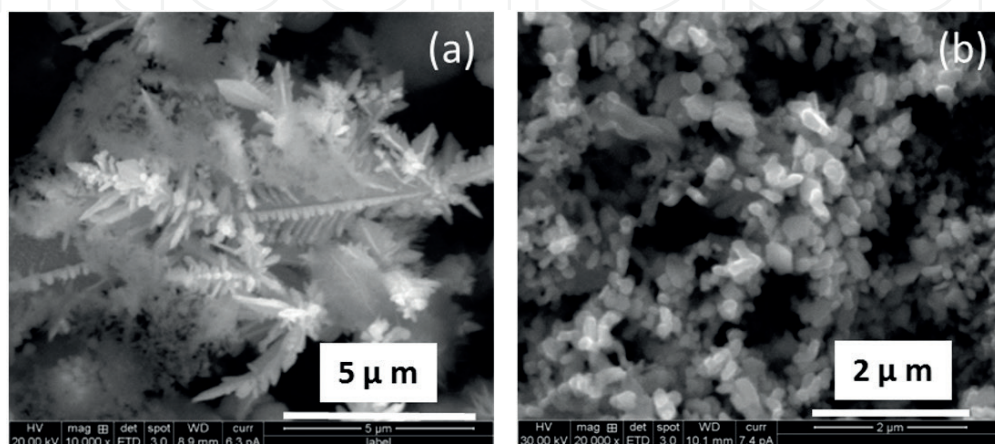


Figure 5. SEM micrograph of Ag-Ni alloy film deposited at 100 mA/cm² and an electrolyte temperature of 80°C for: (a) without thiourea additive and (b) with thiourea additive in the electrolyte [51].

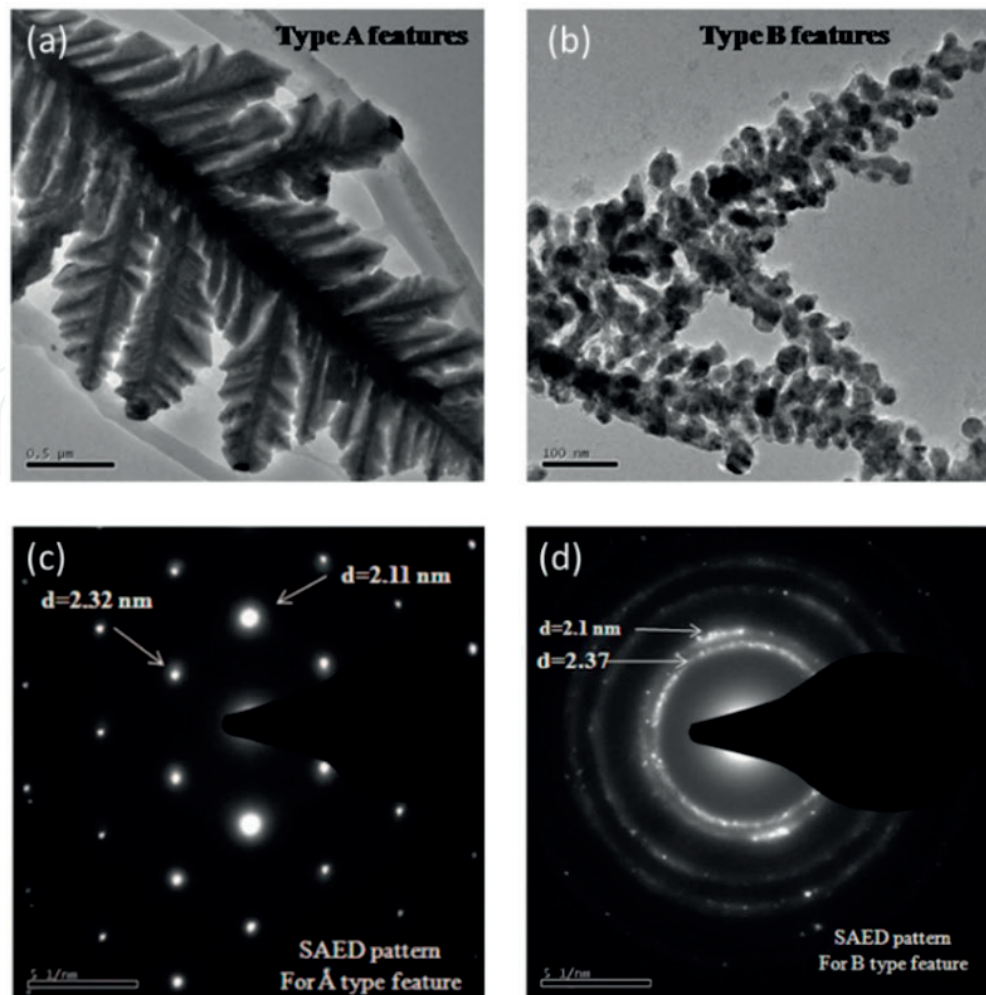


Figure 6. (a and b) TEM bright field image of type A and type B features. (c and d) SAED pattern obtained from type A and type B features [25].

values from the diffraction spots or concentric rings did not match with any of the d-spacing values for standard FCC crystal structures (i.e., Ag and Ni crystal structures). This indicates that the Ag and Ni atoms arranged themselves in solid solution atomic configurations to form a single solid solution of Ag-Ni system. The average size of the nanoparticles in the branched wire type morphology was ~20 nm. It was observed that both features (i.e., type A and type B) contained Ag and Ni atoms in a single solid solution atomic arrangement, but the presence of Ni atoms in the feature made up of ~20-nm-sized particles (i.e., type B) was found to be larger than the type A feature. The greater extent of miscibility of immiscible Ag and Ni atoms in the type B feature can be attributed to the greater curvature provided by the nanoparticles.

IntechOpen

Author details

Brij Mohan Mundotiya^{1*}, Wahdat Ullah² and Krishna Kumar²

1 National Institute of Technology (NIT), Hamirpur, Himachal Pradesh, India

2 Malaviya National Institute of Technology (MNIT), Jaipur, Rajasthan, India

*Address all correspondence to: brij2010iitrke@gmail.com

IntechOpen

© 2018 The Author(s). Licensee IntechOpen. This chapter is distributed under the terms of the Creative Commons Attribution License (<http://creativecommons.org/licenses/by/3.0>), which permits unrestricted use, distribution, and reproduction in any medium, provided the original work is properly cited. 

References

- [1] Burton JJ, Hyman E, Fedak DG. Surface segregation in alloys. *Journal of Catalysis*. 1975;37:106-113. DOI: 10.1016/0021-9517(75)90138-4
- [2] Zhu H, Yang S, Ni G, Yu D, Du Y. Fabrication and magnetic properties of $\text{Co}_{67}\text{Ni}_{33}$ alloy nanowire array. *Scripta Materialia*. 2001;44:2291-2295. DOI: 10.1016/S1359-6462(01)00761-8
- [3] Yamasaki T. High-strength nanocrystalline Ni-W alloys produced by electrodeposition and their embrittlement behaviors during grain growth. *Scripta Materialia*. 2001;44:1497-1502. DOI: 10.1016/S1359-6462(01)00720-5
- [4] Lee W, Lee J, Bae JD, Byun CS, Kim DK. Syntheses of Ni_2Si , Ni_5Si_2 , and NiSi by mechanical alloying. *Scripta Materialia*. 2001;44:97-103. DOI: 10.1016/S1359-6462(00)00547-9
- [5] Yichun L, Jiamin Z, Jikang Y, Jinghong D, Guoyou G, Jianhong Y. Direct electrodeposition of Fe-Ni alloy films on silicon substrate. *Rare Metal Materials and Engineering*. 2014;43:2966-2968. DOI: 10.1016/S1875-5372(15)60043-1
- [6] Torabinejad V, Aliofkhazraei M, Assareh S, Allahyarzadeh MH, Rouhaghdam AS. Electrodeposition of Ni-Fe alloys, composites, and nano coatings—A review. *Journal of Alloys and Compounds*. 2017;691:841-859. DOI: 10.1016/j.jallcom.2016.08.329
- [7] Guo H, Chen Y, Wen R, Yue GH, Peng DL. Facile synthesis of near-monodisperse Ag@Ni core-shell nanoparticles and their application for catalytic generation of hydrogen. *Nanotechnology*. 2011;22(19):195604. DOI: 10.1088/0957-4484/22/19/195604
- [8] Rai RK, Srivastava C. Nonequilibrium microstructures for Ag-Ni nanowires. *Microscopy and Microanalysis*. 2015;21:491-497. DOI: 10.1017/S1431927615000069
- [9] Kabir L, Mandal AR, Mandal SK. Polymer stabilized Ni-Ag and N-Fe alloy nanoclusters: Structural and magnetic properties. *Journal of Magnetism and Magnetic Materials*. 2010;322:934-939. DOI: 10.1016/j.jmmm.2009.11.027
- [10] Van Ingen RP, Fastenau RHJ, Mittemeijer EJ. Formation of crystalline $\text{Ag}_x\text{Ni}_{1-x}$ solid solutions of unusually high supersaturation by laser ablation deposition. *Physical Review Letters*. 1994;72:3116-3119. DOI: 10.1103/PhysRevLett.72.3116
- [11] Lee CC, Chen DH. Large-scale synthesis of Ni-Ag core-shell nanoparticles with magnetic, optical and anti-oxidation properties. *Nanotechnology*. 2006;17:3094-3099. DOI: 10.1088/0957-4484/17/13/002
- [12] Tyler EH, Clinton JR, Luo HL. Electrical resistivity of metastable Ag-Ni alloys. *Solid State Communications*. 1973;13:1409-1411. DOI: 10.1016/0038-1098(73)90178-6
- [13] Mundotiya BM, Srivastava C. Ag-Ni nanoparticles: Synthesis and phase stability. *Electrochemical and Solid-State Letters*. 2012;15(5):K41-K44. DOI: 10.1149/2.esl120008
- [14] Singleton M, Nash P. The Ag-Ni (silver-nickel) system. *Bulletin of Alloy Phase Diagrams*. 1987;8(2):119-121. DOI: 10.1007/BF02873194
- [15] Liu XJ, Gao F, Wang CP, Ishida K. Thermodynamic assessments of the Ag-Ni binary and Ag-Cu-Ni ternary systems. *Journal of Electronic Materials*. 2008;37:210-217. DOI: 10.1007/s11664-007-0315-1
- [16] Li ZC, Liu JB, Li ZF. Interface assisted formation of a metastable hcp

- phase by ion mixing in an immiscible Ag-Ni system. *Journal of Physics: Condensed Matter*. 2000;**12**:9231-9235. DOI: 10.1088/0953-8984/12/44/305
- [17] Zhang Z, Nenoff TM, Huang JY, Berry DT, Provencio PP. Room temperature synthesis of thermally immiscible Ag-Ni nanoalloys. *Journal of Physical Chemistry C*. 2009;**113**:1155-1159. DOI: 10.1021/jp8098413
- [18] Kumar A, Damle C, Sastry M. Low temperature crystalline Ag-Ni alloy formation from silver and nickel nanoparticles entrapped in a fatty acid composite film. *Applied Physics Letters*. 2001;**79**:3314-3316. DOI: 10.1063/1.1414298
- [19] Srivastava C, Chithra S, Malviya KD, Sinha SK, Chattopadhyay. Size dependent microstructure for Ag-Ni nanoparticles. *Acta Materialia*. 2011;**59**:6501-6509. DOI: 10.1016/j.actamat.2011.07.022
- [20] Eom H, Jeon B, Kim D, Yoo B. Electrodeposition of silver-nickel thin films with a galvanostatic method. *Materials Transactions*. 2010;**51**(10):1842-1846. DOI: 10.2320/matertrans.M2010126
- [21] Raghupathy Y, Natarajan KA, Srivastava C. Anti-corrosive and anti-microbial properties of nanocrystalline Ni-Ag coatings. *Materials Science and Engineering B*. 2016;**206**:1-8. DOI: 10.1016/j.mseb.2016.01.005
- [22] Schneider M, Krause A, Ruhn M. Formation and structure of Ni-Ag layer by electrolytic deposition. *Journal of Materials Science Letters*. 2002;**21**:795-797. DOI: 10.1023/A:1015710111396
- [23] Liang D, Liu Z, Hilty RD, Zangari G. Electrodeposition of Ag-Ni films from thiourea complexing solutions. *Electrochimica Acta*. 2012;**82**:82-89. DOI: 10.1016/j.electacta.2012.04.100
- [24] Srivastava C, Mundotiya BM. Electron microscopy of microstructural transformation in electrodeposited Ni-rich Ag-Ni film. *Thin Solid Films*. 2013;**539**:102-107. DOI: 10.1016/j.tsf.2013.05.080
- [25] Srivastava C, Mundotiya BM. Morphology dependence of Ag-Ni solid solubility. *Electrochemical and Solid-State Letters*. 2012;**15**:K10-K15. DOI: 10.1149/2.003202es
- [26] Srivastava C, Mundotiya BM. Size and solid solubility in electrodeposited Ag-Ni nanoparticles. *Materials Science Forum*. 2013;**736**:21-26. DOI: 10.4028/www.scientific.net/MSF.736.21
- [27] Bona AD. Characterizing ceramics and the interfacial adhesion to resin: II—The relationship of surface treatment, bond strength, interfacial toughness and fractography. *Journal of Applied Oral Science*. 2005;**13**:101-109. DOI: 10.1590/S1678-77572005000200002
- [28] Cao G. *Nanostructures and Nanomaterials: Synthesis, Properties, and Applications*. London: World Scientific; 2004. 175 p. DOI: 10.1142/9781860945960_0005
- [29] Paunovic M, Schlesinger M, Snyder DD. Fundamental considerations. In: Schlesinger M, Paunovic M, editors. *Modern Electroplating*. 5th ed. New Jersey: Wiley; 2011. pp. 1-32. DOI: 10.1002/9780470602638
- [30] Markov IV. *Crystal Growth for Beginners: Fundamentals of Nucleation, Crystal Growth and Epitaxy*. 2nd ed. Singapore: World Scientific; 1995. 422 p. DOI: 10.1142/9789812386243_0003
- [31] US Water System. *Deionized Water vs Distilled Water*. 2018. Available from: <https://www.uswatersystems.com/deionized-water-vs-distilled-water>. [Accessed: 2018-06-27]

- [32] Santhi K, Karthick SN, Kim H, Nidhin M, Narayanan V, Stephen A. Microstructure analysis of the ferromagnetic Ag-Ni system synthesized by pulsed electrodeposition. *Applied Surface Science*. 2012;**258**:3126-3132. DOI: 10.1016/j.apsusc.2011.11.049
- [33] Gomez E, Garcia-Torres J, Valles E. Study and preparation of silver electrodeposits at negative potentials. *Journal of Electroanalytical Chemistry*. 2006;**594**:89-95. DOI: 10.1016/j.jelechem.2006.05.030
- [34] Kamel MM. Anomalous codeposition of Co-Ni: Alloys from gluconate baths. *Journal of Applied Electrochemistry*. 2007;**37**:483-489. DOI: 10.1007/s10800-006-9279-8
- [35] Qu NS, Zhu D, Chan KC, Lei WN. Pulse electrodeposition of nanocrystalline nickel using ultra narrow pulse width and high peak current density. *Surface and Coatings Technology*. 2003;**168**:123-128. DOI: 10.1016/S0257-8972(03)00014-8
- [36] Sharma A, Das S, Das K. Pulse electroplating of ultrafine grained tin coating. In: Aliofkhaezrai M, editor. *Electroplating of Nanostructures*. Intech Open; 2015. pp. 105-129. DOI: 10.5772/61255
- [37] Ibl N. Some theoretical aspects of pulse electrolysis. *Surface Technology*. 1980;**10**:81-104. DOI: 10.1016/0376-4583(80)90056-4
- [38] Watanabe T. *Nano-Plating Microstructure Control Theory of Plated Film and Data Base of Plated Film Microstructure*. Oxford, UK: Elsevier Ltd; 2004
- [39] Sharma A, Bhattacharya S, Das S, Das K. A study on the effect of pulse electrodeposition parameters on the morphology of pure tin coatings. *Metallurgical and Materials Transactions A*. 2014;**45**:4610-4622. DOI: 10.1007/s11661-014-2389-8
- [40] Weissmueller J, Bunzel P, Wilde G. Two-phase equilibrium in small alloy particles. *Scripta Materialia*. 2004;**51**:813-818. DOI: 10.1016/j.scriptamat.2004.06.025
- [41] Bellomo A, De Marco D, De Robertis A. Formation and thermodynamic properties of complexes of Ag(I) with thiourea as ligand. *Talanta*. 1973;**20**:1225-1228. DOI: 10.1016/0039-9140(73)80088-8
- [42] Bdikin IK, Strukova GK, Strukov GV, Kedrov VV, Matveev DV, Zer'kov SA, et al. Growth, crystal structure and stability of Ag-Ni/Cu films. *Materials Science Forum*. 2006;**514-516**:1166-1170. DOI: 10.4028/www.scientific.net/MSF.514-516.1166
- [43] Burstein GT. A hundred years of Tafel's equation: 1905-2005. *Corrosion Science*. 2005;**47**:2858-2870. DOI: 10.1016/j.corsci.2005.07.002
- [44] Tan AC. *Tin and Solder Plating in the Semiconductor Industry: A Technical Guide*. 1st ed. London: Chapman & Hall; 1993. 326 p. ISBN: 0442317123
- [45] Inamdar AI, Mujawar SH, Barman SR, Bhosale PN, Patil PS. The effect of bath temperature on the electrodeposition of zinc oxide thin films via an acetate medium. *Semiconductor Science and Technology*. 2008;**23**:085013. (6pp). DOI: 10.1088/0268-1242/23/8/085013
- [46] Rashidi AM, Amadeh A. Effect of electroplating parameters on microstructure of nanocrystalline nickel coatings. *Journal of Material Science and Technology*. 2010;**26**:82-86. DOI: 10.1016/S1005-0302(10)60013-8
- [47] Sahaym U, Miller SL, Norton MG. Effect of plating temperature on Sn surface morphology. *Materials Letters*. 2010;**64**:1547-1550. DOI: 10.1016/j.matlet.2010.04.036

[48] Garcia-Torres J, Valles E, Gomez E. Influence of bath temperature and bath composition on Co-Ag electrodeposition. *Electrochimica Acta*. 2010;**55**:5760-5767. DOI: 10.1016/j.electacta.2010.05.014

[49] Gomez H, Lizama H, Suarez C, Valenzuela A. Effect of thiourea concentration on the electrochemical behavior of gold and copper electrodes in presence and absence of Cu(II) ions. *Journal of the Chilean Chemical Society*. 2009;**54**:439-444. DOI: 10.4067/S0717-97072009000400026

[50] Schmidt WU, Alkire RC, Gewirth AA. Mechanic study of copper deposition onto gold surfaces by scaling and spectral analysis of in-situ atomic forces microscopic images. *Journal of the Electrochemical Society*. 1996;**143**:3122-3132. DOI: 10.1149/1.1837174

[51] Mundotiya BM. Phases and morphology in electrodeposited Ag-Ni film and nano-sized particles [thesis]. Indian Institute of Science Bangalore: Bangalore; 2012

IntechOpen